Journal of Power Sources 192 (2009) 2–13

Contents lists available at ScienceDirect

Journal of Power Sources

journal homepage: www.elsevier.com/locate/jpowsour

Effect of DC current polarization on the electrochemical behaviour of $La_2NiO_{4+\delta}$ and $La_3Ni_2O_{7+\delta}$-based systems☆

D. Pérez-Coll[a,*], A. Aguadero[a], M.J. Escudero[a], L. Daza[a,b]

[a] Centro de Investigaciones Energéticas, Medioambientales y Tecnológicas (CIEMAT), Av. Complutense 22, 28040 Madrid, Spain
[b] Instituto de Catálisis y Petroleoquímica (CSIC), C/ Marie Curie 2, Campus Cantoblanco, 28049 Madrid, Spain

ARTICLE INFO

Article history:
Received 3 October 2008
Received in revised form 23 October 2008
Accepted 24 October 2008
Available online 31 October 2008

Keywords:
IT-SOFC
Lanthanum nickel oxides
Cathode performance
Current polarization
Impedance Spectroscopy

ABSTRACT

The electrode performance of La_2NiO_4 and $La_3Ni_2O_7$ as cathode materials for solid oxide fuel cells (SOFC) was analyzed. The study was focused on the electrode polarization resistance of the interfaces formed by the cathodes with $Ce_{0.8}Sm_{0.2}O_{2-\delta}$ + 2%Co electrolyte. The study was extended to cathodes based on La_2NiO_4–$Ce_{0.8}Sm_{0.2}O_{2-\delta}$ composite and Pt to analyze the effect of changing the electronic and/or ionic transport properties on the electrode interface resistance. The electrode performance was studied in open circuit conditions and with DC current polarization. Important differences in the performance of the pure cathode materials were obtained as function of DC current flux. However, in La_2NiO_4–$Ce_{0.8}Sm_{0.2}O_{2-\delta}$ composite the DC current flux produces minor changes in the electrode polarization resistance. The aging process also affects the OCV electrode performance of cathodes based on Pt and pure ceramics, whereas the effect is practically invaluable in La_2NiO_4–$Ce_{0.8}Sm_{0.2}O_{2-\delta}$ composite. The electrode performance is higher for the composite cathode compared to pure ceramic electrodes for OCV or for low values of DC polarization. However, the important decrease in the interface resistance obtained for high values of DC current flux for La_2NiO_4 and $La_3Ni_2O_7$ cathodes increases their electrode performances to values close to those obtained in La_2NiO_4–$Ce_{0.8}Sm_{0.2}O_{2-\delta}$ composite. This retains the cathode overpotential with values as low as 140 mV at 750 °C for values of current load of 530 mA cm^{-2} for both pure and composite La_2NiO_4-based cathodes. The low cathode overpotential allows to estimate values of power density between 300 and 350 mW cm^{-2} at 750 °C for La_2NiO_4, $La_3Ni_2O_7$ and La_2NiO_4–$Ce_{0.8}Sm_{0.2}O_{2-\delta}$ composite, operating with $Ce_{0.8}Sm_{0.2}O_{2-\delta}$ + 2%Co electrolyte, with 300 μm in thickness, and a Ni–$Ce_{0.8}Sm_{0.2}O_{2-\delta}$ cermet anode with H_2 as fuel.

1. Introduction

Reducing the operating temperature in SOFC from the traditional high temperatures (~1000 °C) to intermediate temperatures (<800 °C) is one of the more interesting features to make viable the SOFC technology [1–2]. The main advantages coming from the decrease in the operating temperature are the possible use of inexpensive materials and the suppression of reactions between the cell components [3]. However this low/intermediate temperature produces an important decrease in the performance of the cell, mainly due to the relatively high internal resistances coming from the electrolyte and the interface cathode/electrolyte [4,5]. The decrease in these internal resistances is essential to make SOFCs economically competitive. Diminishing the electrolyte thickness is the way to reduce the internal loss of the electrolyte, whereas the cathode/electrolyte interface should be improved by the use of mixed conducting cathodes or the addition of an ionically conducting second phase to the electronically conducting cathode [6,7]. However some difficulties to develop better SOFC components arise from the complexity of the electrochemical processes involved. In particular the oxygen reduction reaction at the cathode is usually considered the main limiting factor in SOFC systems but its mechanistic understanding is still unsatisfactory [8]. This makes difficult to get consistent set of values for cathode losses from the literature [9,10] and important discrepancies can be obtained from results coming from different authors [11,12]. The main reason for most discrepancies could be related to microstructural differences associated to the use of porous electrodes. These porous systems give realistic information of materials in SOFC conditions but it is very difficult to separate microstructural/morphological properties from intrinsic properties [8]. On the other hand, the electrode polarization resistance is usually measured under OCV conditions, which is difficult to relate to electrode overpotential under working conditions.

☆ Presented at CONAPPICE 2008, Zaragoza, Spain, 24–26 September 2008.

* Corresponding author. Tel.: +34 913 466 622; fax: +34 913 466 269.
E-mail addresses: domingo.perez@ciemat.es, dpcoll@ull.es (D. Pérez-Coll).

0378-7753/$ – see front matter © 2008 Elsevier B.V. All rights reserved.
doi:10.1016/j.jpowsour.2008.10.073

In this way, several authors have reported a considerably decrease in the interfacial resistance of the cathode/electrolyte interface due to DC polarization for some cathode materials [10,13,14]. In general, they have attributed this improvement to some processes of reduction of the cathode material and the consequent creation of oxygen vacancies when DC current is fluxing (e.g. reduction of Mn^{3+} to Mn^{2+} in LSM-based cathodes) [10,14]. However it has been shown that the mechanism by which current polarization enhances the cathode performance is only partly understood. In particular McIntosh et al. [10] analyzed the system based on LSM–YSZ composite cathode over YSZ electrolyte and they found that the OCV resistance of the interface cathode/electrolyte decreased when previously polarized by high current densities. Moreover they required periods of many hours or even days to relax to the starting interfacial resistance, pointing out that changes in oxidation states could be the not only reason for the obtained changes in performances, given that these kinds of processes typically possess relax time scales of minutes. Thus the study of interface cathode/electrolyte under DC cathodic polarization needs further investigations and also needs to be extended to different cathode and electrolyte materials.

In recent years the interest in the K_2NiF_4 type oxides has increased considerably, due to the mixed electronic and ionic transport properties in oxidizing conditions [15–17], which is a very interesting feature to use as cathode in SOFC. The overstoichiometry in $La_2NiO_{4+\delta}$ promotes the oxygen conductivity, and the electronic properties exhibit a transition from metal to semiconductor-type, from high to low temperatures, respectively, displaying a maximum of 82 S cm^{-1} around 400 °C [15,18]. On the other hand, the OCV interfacial resistance is highly dependent on the nature of the interface formed by the cathode with the corresponding electrolyte, as it was confirmed in ceria-based electrolytes [19]. In the system based on $Ce_{1-x}Sm_xO_{2-\delta}$, the use of electrolytes with composition $Ce_{0.8}Sm_{0.2}O_{2-\delta}$ + 2%Co showed the best performance in OCV conditions when used with La_2NiO_4, and it was improved by the use of La_2NiO_4–$Ce_{0.8}Sm_{0.2}O_{2-\delta}$ composite as cathode. However, it has been observed some instability of $La_2NiO_{4+\delta}$ after long time at 800 °C due to the formation of Ni^{2+}/Ni^{3+} secondary phases [20]. Moreover, it was evidenced a slight formation of $La_3Ni_2O_{7+\delta}$ as secondary phase when using $La_2NiO_{4+\delta}$–$Ce_{0.8}Sm_{0.2}O_{2-\delta}$ composite and $La_2Ni_{0.9}Co_{0.1}O_{4+\delta}$ as cathodes with lanthanide-doped ceria electrolytes [19,21]. This oxidized $La_3Ni_2O_7$ could affect the cathode performance during the cell operation after long times of measurements.

In this work, we investigated the electrode/electrolyte polarization properties of cathodes based on Ruddlesden–Popper systems La_2NiO_4 and $La_3Ni_2O_7$ over $Ce_{0.8}Sm_{0.2}O_{2-\delta}$ + 2%Co electrolyte when DC current is fluxing through the samples. Processes were also analyzed before and after DC polarization aging to understand the electrochemical processes of the oxygen reaction. In the study we also carefully analyzed differences coming from the use of symmetrical and 3-probe configurations in OCV conditions and with simultaneous DC current flux. Also we induced important modifications in the electrode properties by the introduction of an ionically conducting phase ($Ce_{0.8}Sm_{0.2}O_{2-\delta}$) as composite. Moreover we paid attention to Pt electrodes without ceramic phase as an ideal electronic conductor and the effect of current density flux on the electrode performance was also studied.

2. Experimental

2.1. Synthesis

Powders of La_2NiO_4 and $La_3Ni_2O_7$ were prepared by nitrate–citrate synthesis route [19–22]. Stoichiometric amounts of La_2O_3 and $Ni(NO_3)_2{\cdot}6H_2O$ (Panreac, 99%) were dissolved in citric acid (Panreac, 10%) with some drops of HNO_3 (Panreac, 65%) with continuous stirring. The obtained solutions were slowly evaporated to get an organic gel which was dried at 120 °C and slowly calcined at 600 °C to decompose the organic phases. In order to obtain the La_2NiO_4 phase, the powders were calcined at 950 °C for 8 h and slowly cooled down to room temperature. A preliminary heat treatment of 900 °C for 2 h followed by 1150 °C for 12 h leads to the formation of the $La_3Ni_2O_7$ compound with low crystallinity. A pure well-crystallized $La_3Ni_2O_7$ phase was obtained after calcining at 1150 °C for 48 h. XRD measurements (Philips X'Pert-MPD) were performed to obtain the identification of the phases and their crystalline purity. Lattice parameters were extracted from Rietveld refinement of XRD patterns using Winplotr and Fullprof suite [23,24].

As electrolytes we used powders of $Ce_{0.8}Sm_{0.2}O_{2-\delta}$ (Praxair, 99.9%) (20CSO) doped with 2 mol% of cobalt to improve the sinterability at low temperature [25,26]. For this purpose the powders were impregnated with an ethanol solution of $Co(NO_3)_2{\cdot}6H_2O$, milled until dry and calcined at 650 °C for 1 h. Composites of La_2NiO_4 and $Ce_{0.8}Sm_{0.2}O_{2-\delta}$ were also prepared with a respective ratio of 2:1, w:w, to use as cathode (La_2NiO_4–20CSO). XRD measurements were performed to analyze the crystalline structure of the powders.

2.2. Preparation of the cells and microstructural characterization

Electrolyte pellets of about 20 mm in diameter and 1.3 mm in thickness were prepared by pressing the powders of $Ce_{0.8}Sm_{0.2}O_{2-\delta}$ + 2%Co (20CSO2Co) and sintering at 1150 °C for 10 h. This provided samples with 95–96% of the theoretical density. Electrochemical cells were prepared in symmetrical configuration and in 3-probe set-up with an external reference electrode (Fig. 1). The study was focused on cathodes based on La_2NiO_4, $La_3Ni_2O_7$, La_2NiO_4–20CSO and Pt. Ball milled cathode materials (except Pt electrode) were mixed with Decoflux (Decoflux™, WB41, Zschimmer and Schwartz) and placed over the electrolytes by painting and calcining at 1000 °C for 4 h. Pt paste was painted over the cathode materials to ensure equipotential conditions and to act as current collector. In the 3-probe configuration Pt was also employed as a reference electrode located around the working electrode (Fig. 1). Working and counter electrodes were symmetrically placed with 6 mm in diameter and the external electrode was located at a distance larger than three-electrolyte thickness from the edge of active electrodes, to ensure no current fluxes towards the reference [27]. For electrochemical measurements the reference electrode was placed with the counter electrode in the symmetrical configuration, and on the external Pt electrode for the 3-probe semi-cell measurements (Fig. 1).

Scanning electron microscopy (SEM, Hitachi S-2500) was performed on cathode surfaces to analyze the morphology and microstructure of the cathodes. In order to analyze the chemical compatibility of cathodes and electrolytes, XRD measurements were performed in cathode materials after being applied with the binder over the electrolyte pellets and calcined in the cell at 1000 °C for 4 h.

2.3. Electrochemical measurements

Electrode characterization was mainly performed by impedance spectroscopy in air using a Frequency Response Analyzer (Autolab PGSTAT 302, Eco Chemie). Experimental measurements were performed in galvanostatic mode in the range of 10^{-2} to 10^6 Hz with an excitation signal of 5 mA, and decreasing the temperature from 1000 to 500 °C. Electrode performance was analyzed under open

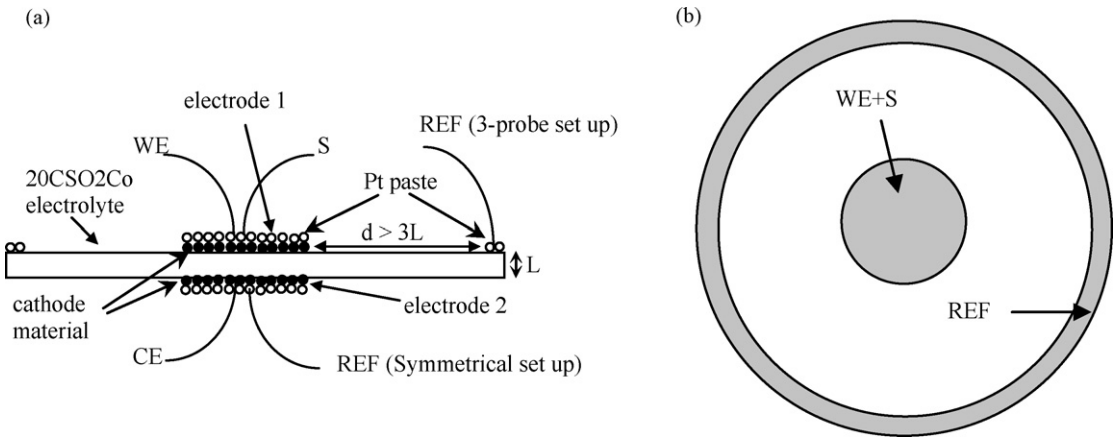

Fig. 1. Experimental set-up employed for the electrochemical characterization. Reference electrode was placed with the counter electrode in symmetrical configuration and on the external Pt electrode in the 3-probe configuration. (a) Transversal view and (b) top view.

circuit voltage (OCV) and under DC current fluxes ranged from 35 to 530 mA cm^{-2} between the working and the counter electrodes. DC current fluxes were also applied for different steps of time and the corresponding values of DC voltage were recorded. Then OCV impedance spectroscopy measurements were performed after DC current fluxes to analyze the effect of the electrochemical history on the interfacial resistance. Reference electrode was turned from the counter electrode to the outsider electrode to compare symmetrical and 3-probe configurations. The effect was also analyzed using Pt as active electrode. Impedance spectra were fitted to equivalent circuits using Zview 2.9c software (Scribner Associates).

3. Results and discussion

3.1. Structure and microstructure characteristics

XRD results of La_2NiO_4 and $La_3Ni_2O_7$ powders confirmed the presence of pure and well-crystallized Ruddlesden–Popper $La_{n+1}Ni_nO_{3n+1}$ (n = 1 and 2) structures (Fig. 2). Rietveld refinement was performed on XRD data in order to obtain the structural parameters of each compound. The orthorhombic *Fmmm* space group was chosen to describe the crystal structures at room temperature in agreement with other X-ray diffraction studies in the literature [22,20]. Table 1 summarizes the unit-cell parameters obtained. XRD results of 20CSO2Co powders calcined at 650 °C showed the presence of pure fluorite single phase with no appreciable secondary phases. Powders calcined at 1150 °C for 10 h improve the crystallinity compared with samples calcined at low temperature. Previous results of Rietveld refinement [19] confirmed that the unit cell parameter of 20CSO2Co sintered at 1150 °C is preserved compared with pure 20CSO sintered at 1600 °C. This indicated low solubility of cobalt in the as doped fluorite structure.

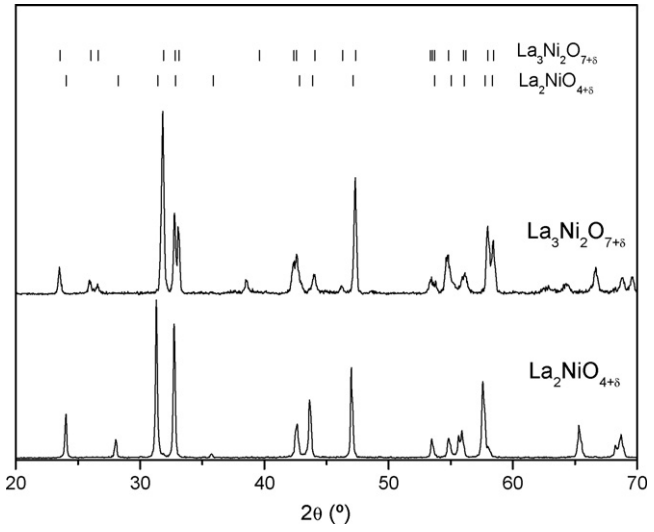

Fig. 2. X-ray diffraction patterns of as prepared $La_2NiO_{4+\delta}$ and $La_3Ni_2O_{7+\delta}$.

The analysis of chemical stability between La_2NiO_4 and $La_3Ni_2O_7$ with 20CSO2Co confirmed no significant reaction when the cathodes are placed over the electrolyte and calcined at 1000 °C for 4 h. However, there is a slight reaction between $La_2NiO_{4+\delta}$ and 20CSO in the composites $La_2NiO_{4+\delta}$–20CSO (2:1; w:w) when they are previously mixed, placed on the electrolyte and heated at 1000 °C for 4 h, leading to the minor formation of the Ruddlesden–Popper $La_3Ni_2O_7$ as a secondary phase as we have previously reported [19]. Other authors have observed the formation of more oxidized Ruddlesden–Popper, $La_3Ni_2O_7$ and $La_4Ni_3O_{10}$ impurity phases when La_2NiO_4 is heated for long periods of time [20]. The formation of these impurity phases could be favoured when mixing the cathode with a ceria-based powder due to the possible diffusion of La^{3+} to the ceria-based phase leading to a "La-deficient" oxide. The impoverishment in La would provoke the partial transformation of La_2NiO_4 to La-deficient phases such as $La_3Ni_2O_7$ and $La_4Ni_3O_{10}$ [28].

Fig. 3(a) and (b) shows SEM images of La_2NiO_4 and La_2NiO_4–20CSO cathode surfaces, respectively, after placed over 20CSO2Co electrolyte and calcined at 1000 °C for 4 h. The powders are homogeneously distributed and no important differences in porosity are observed. Fig. 3(c) and (d) shows the microstructure obtained for La_2NiO_4 and La_2NiO_4–20CSO after the cells were cathodically polarized with a DC current flux of 354 mA cm^{-2} for 160 min at 800 °C. It is observed that the DC current polarization does not produce appreciable changes in the microstructure of the cathodes, and the homogeneity and porosity is mainly preserved. It is to note that the microstructure of Pt current collectors is considerably affected by the aging and there is an important decrease in

Table 1
Unit cell parameters of $La_{n+1}Ni_nO_{3n+1}$ (n = 1, 2) refined in the *Fmmm* space group from XRD data.

Sample	a (Å)	b (Å)	c (Å)	V (Å^3)
$La_2NiO_{4+\delta}$	5.45378(3)	5.45904(3)	12.68328(6)	377.612(3)
$La_3Ni_2O_{7+\delta}$	5.39905(6)	5.45260(6)	20.5420(3)	604.74(1)

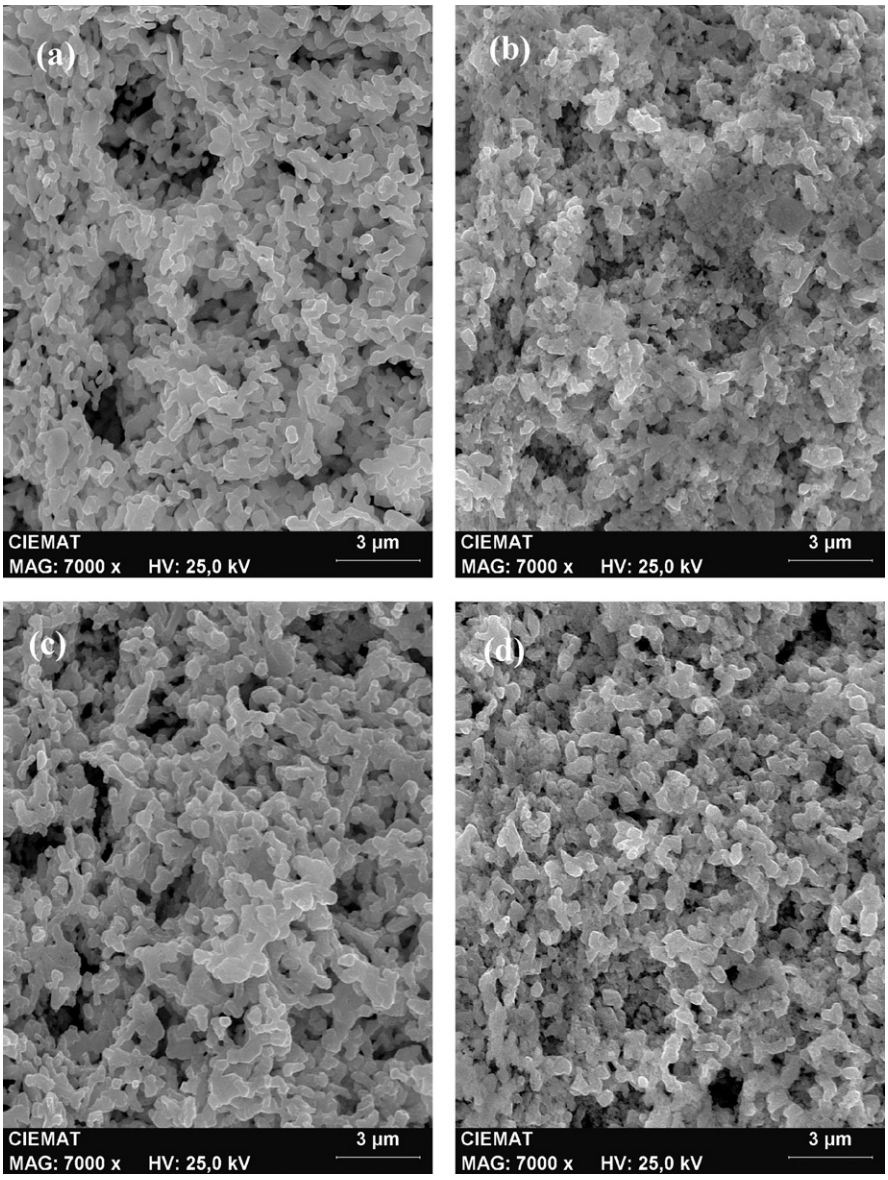

Fig. 3. Scanning electron microscopy of La_2NiO_4, (a) and (c), and La_2NiO_4–20CSO, (b) and (d), deposited over 20CSO2Co and calcined at 1000 °C for 4 h. Panels (a) and (b) were obtained before the electrochemical measurements, and (c) and (d) after applying a cathodic current of 354 mA cm^{-2} for 160 min at 800 °C.

the effective area when the time of exposition to high temperature increases (coarsening). This could be responsible of a decrease in the electrode performance with time.

3.2. Impedance analysis under OCV conditions

Fig. 4 shows the impedance spectra obtained under OCV conditions for the $La_3Ni_2O_7$ cathode with the 20CSO2Co electrolyte at 800 °C. Results show the electrode polarization processes obtained in symmetrical and 3-probe configurations. In the last measurements the working and counter electrodes were interchanged to analyze the process in each of the electrodes of the symmetrical configuration (electrodes 1 and 2 in Fig. 1). The obtained spectra reveal an ohmic contribution at high frequencies, mainly due to the electrolyte resistance (R_s), and two or three overlapped semicircles at lower frequencies associated to the interface polarization processes. Note that in the spectra shown in Fig. 4, the electrolyte resistance was subtracted for a clearer comparison of the electrode processes. At high frequencies it is also observed an inductive process arising from the electrochemical equipment and Pt wires. Impedance spectra were fitted to parallel resistance (R_p)-constant phase (CPE_p) elements associated in series to account each semicircle contribution. Ohmic resistance and external inductance were fitted by the introduction of series resistance (R_s) and inductance (L) (Fig. 4). Each resistance and capacitance processes (extracted from the R_p-CPE_p fitted values) allowed to obtain relaxation frequencies of each polarization contribution which are separated in orders of magnitude.

In symmetrical configuration, the spectra show the contribution associated to the total ohmic resistance of the electrolyte and the interface polarization of the two electrodes used as working and counter electrodes. However in our 3-probe set-up (Fig. 1) the reference electrode is placed in an equipotential inactive zone of the electrolyte which avoids potential losses in the reference. This implies that the interface polarization process is only due to the polarization of the working electrode. On the other hand, electrolyte ohmic loss is only associated to one half of the electrolyte thickness given that the potential between working and reference

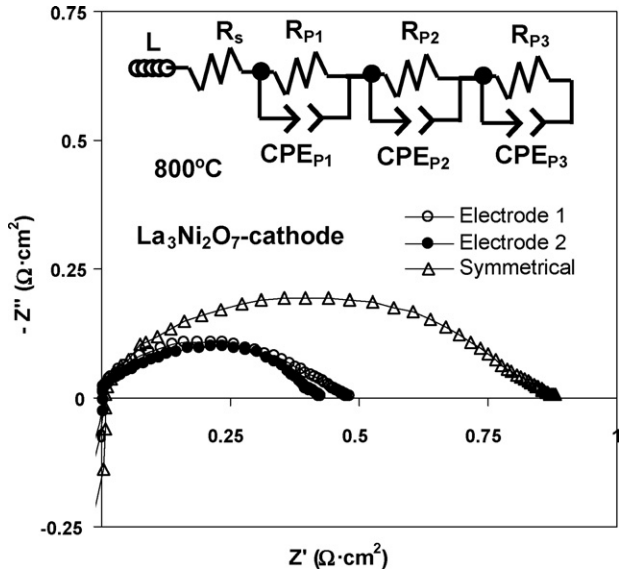

Fig. 4. Impedance spectra in OCV conditions for $La_3Ni_2O_7$ cathode with 20CSO2Co electrolyte at 800 °C, and equivalent circuit used for the fitting of the spectra. Results obtained using symmetrical and 3-probe configurations are presented.

electrodes is one half of the potential between working and counter electrodes [27].

In Fig. 4, the polarization of both electrodes (electrodes 1 and 2), measured by interchanging the working and counter electrodes in 3-probe configuration, is 0.48 and 0.43 Ω cm^2 for electrodes 1 and 2, respectively, which indicates similar microstructure properties of both electrodes. Results obtained in symmetrical configuration are in good agreement with results of each electrode contribution, and the averaged electrode performance is 0.44 Ω cm^2. These results obtained in the $La_3Ni_2O_7$ electrode are mainly reproduced in the other cathode materials. Some differences were obtained between symmetrical and 3-probe measurements (e.g. using Pt electrodes) caused by some differences in results obtained in each of the electrodes, probably due to some differences in microstructural properties. These results indicate that in OCV conditions the symmetrical configuration shows good results of the electrode polarization only if the microstructure of both electrodes is approximately identical.

Fig. 5 shows a comparison of the OCV spectra at 800 °C for different electrodes used with 20CSO2Co electrolyte, obtained in 3-probe configuration in air conditions. It is clearly observed that the use of ceramic materials as cathode improves the electrode performance compared to Pt metallic electrode, whereas La_2NiO_4 improves the

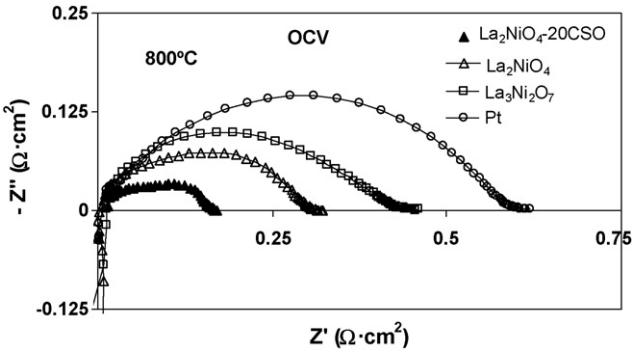

Fig. 5. Electrode performances of Pt, $La_3Ni_2O_7$, La_2NiO_4 and La_2NiO_4–20CSO cathodes placed over 20CSO2Co electrolyte in OCV conditions and 3-probe configuration.

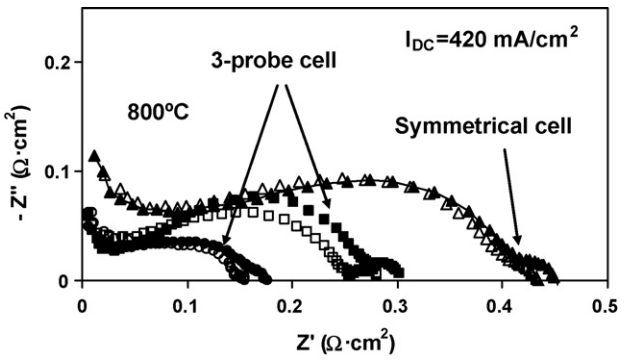

Fig. 6. Electrode polarization at 800 °C of $La_3Ni_2O_7$ cathode placed over 20CSO2Co in symmetrical configuration (triangles) and 3-probe configuration (squares and circles) under DC current flux of 420 mA cm^{-2}. Working electrode was cathodically (squares and open triangles) and anodically (circles and closed triangles) polarized. In 3-probe configuration open symbols correspond to electrode 1 and closed symbols to electrode 2. Note that in symmetrical configuration it is represented the total contribution of the two electrodes.

performance compared to $La_3Ni_2O_7$. It is to note that the average grain size of La_2NiO_4 is sensibly lower than that of $La_3Ni_2O_7$, due to the lower temperature employed in the synthesis process. This could be the responsible of the better performance obtained for La_2NiO_4, given that the active surface of reaction is increased. It is also appreciated that the composite La_2NiO_4–20CSO produces the best performance of the studied materials, due to the introduction of the ionically conducting phase (20CSO) enlarges the active places of reaction beyond the interface cathode/electrolyte.

3.3. Symmetrical and 3-probe configurations under DC current flux

The electrode polarization process was also analyzed under fluxes of DC current. Fig. 6 shows the spectra obtained at 800 °C for $La_3Ni_2O_7$ cathode in symmetrical and 3-probe configurations under a current density flux of 420 mA cm^{-2}. The electrolyte ohmic contribution is not affected by the current flux, as it is observed in its estimated ionic conductivity presented in Fig. 7. However, the spectra reveal the presence of artifacts at high frequencies introduced by our FRA system, which were previously observed for LSM–YSZ composite cathode over YSZ electrolyte [9], and even for $Nd_{1.95}NiO_{4+\delta}$ electrodes over YSZ electrolyte [29]. The total elec-

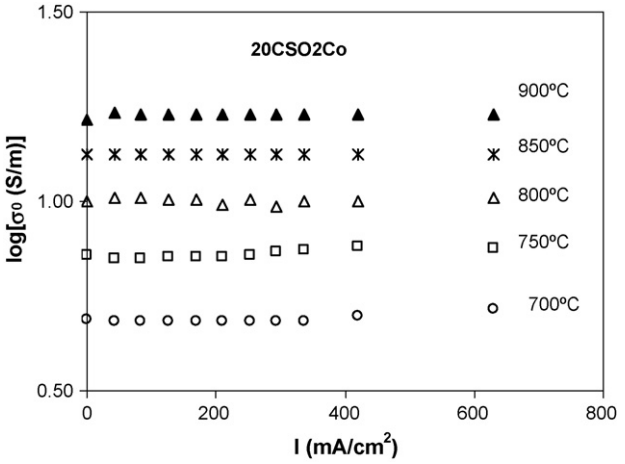

Fig. 7. Electrolyte conductivity of 20CSO2Co as a function of current density, obtained by the series contribution (R_s) of the system $La_3Ni_2O_7$/20CSO2Co and taking into account the semi-cell conditions in 3-probe configuration.

trode polarization in symmetrical configuration (contribution of both electrodes) was improved from 0.88 Ω cm^2 for OCV conditions (Fig. 4) to 0.45 Ω cm^2 under 420 mA cm^{-2} (Fig. 6). Impedance spectra shown in Fig. 6 were obtained for the working electrode under both cathodic (−420 mA cm^{-2}) and anodic (+420 mA cm^{-2}) DC polarization. When the working electrode is cathodically polarized, the oxygen reduction reaction takes place at the working electrode whereas the oxygen oxidation reaction takes place at the counter electrode. When the working electrode is anodically polarized the oxygen reactions at the working and counter electrodes are reversed. Fig. 6 shows that in symmetrical configuration the total polarization of two electrodes is independent on the current direction given that both electrodes compensate possible differences arisen from the different oxygen reactions. The study of the polarization of each electrode, performed using 3-probe configuration (Fig. 6) reveals that the cathode material possesses different performances under cathodic and anodic polarization. In particular, results obtained when the working electrode is cathodically polarized possess higher values of interface resistance compared with the anodic polarization. On the other hand, the results obtained by interchanging the WE and CE from electrodes 1 and 2, respectively, reveals that both electrodes possess similar properties under similar conditions of current polarization. These results reveal that the measurements obtained under symmetrical configuration do not give adequate values of cathode polarization when DC current is fluxing. This is due to the fact that the symmetrical configuration gives the values obtained for both electrodes, one of them cathodically polarized and the other one anodically polarized, which possess different performances. This is confirmed by the results in Fig. 6, in which the total electrode resistance of the symmetric cell (∼0.45 Ω cm^2) is the sum of the resistances of one electrode under cathodic polarization and the other one under anodic polarization. The study of 420 mA cm^{-2} anodically and cathodically supplied to the working electrode was also performed for the other materials, leading to similar conclusions that the performance under anodic polarization was always higher than that obtained under cathodic polarization. However for the study of the cathode materials to be used in SOFC conditions the working electrode should be cathodically polarized to produce the oxygen reduction reaction. It is important to note that after impedance measurements with DC current flux, the original nonpolarized state was returned in OCV conditions.

3.4. Impedance studies varying DC current flux

The effect of DC current flux on the electrode polarization presented below was analyzed by impedance spectroscopy in 3-probe configuration with the working electrode under cathodic polarization. Fig. 8 shows the spectra at 700 °C obtained for La_2NiO_4 cathode (Fig. 8(a)) and La_2NiO_4–20CSO composite cathode (Fig. 8(b)) over 20CSO2Co electrolyte. The spectra again reveal the presence of artifacts at high frequencies, as it was observed before (Fig. 6). In addition, inductive loops were also formed at very low-frequencies [9,30], which were eliminated from the spectra for better comparison of electrode processes.

Results of pure cathode (Fig. 8(a)) show that the performance of the electrode obtained under OCV conditions is clearly improved in current flux conditions. It is also appreciated that there is an increase in the performance when the current flux increases, and the electrode polarization resistance is enormously decreased from 3.30 Ω cm^2 for OCV to 0.32 Ω cm^2 for 530 mA cm^{-2}. This improvement in the performance of the electrode with the current flux is very important in order to decrease the internal loss of the cell for high values of current density in a SOFC. The use of composite as cathode (La_2NiO_4–20CSO) clearly improves the performance

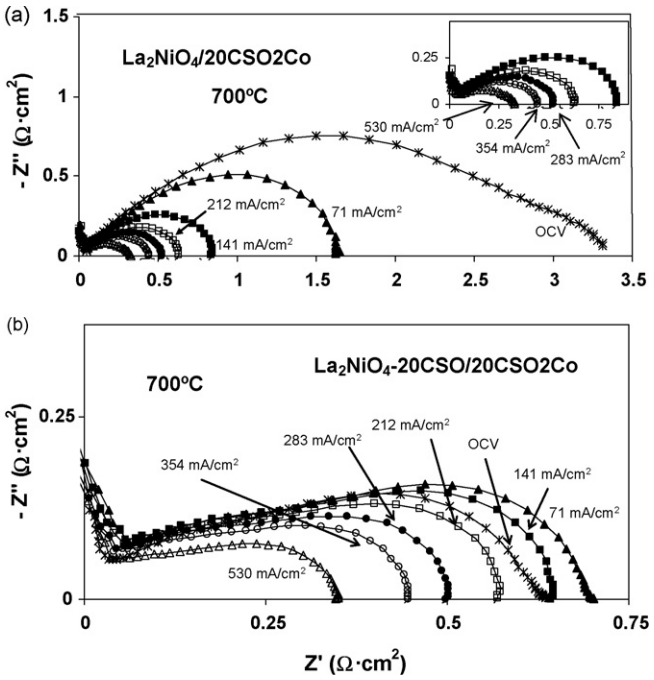

Fig. 8. Impedance spectra at 700 °C of La_2NiO_4 (a) and La_2NiO_4–20CSO (b) cathodes over 20CSO2Co electrolytes for different values of current density between the working and the counter electrodes. Measurements were performed in 3-probe configuration and the working electrode was cathodically polarized.

in OCV conditions compared to the pure cathode (Fig. 8(b)). However, the performance obtained at 700 °C in OCV conditions is harmed for small fluxes of current densities (71 and 141 mA cm^{-2}) whereas is progressively increased for higher current fluxes. The electrode polarization for La_2NiO_4–20CSO is only decreased from 0.64 Ω cm^2 for OCV to 0.34 Ω cm^2 for 530 mA cm^{-2}. This surprising result reveal that the enormous improvement in the cathode performance for the composite compared to pure material in OCV conditions, completely disappears for high current densities fluxes (e.g. 530 mA cm^{-2}).

The effect analyzed above at 700 °C is not uniformly obtained for different temperatures as it is observed in Fig. 9 for the interface polarization as a function of DC current density at different temperatures, for cathodes of La_2NiO_4, $La_3Ni_2O_7$, La_2NiO_4–20CSO and Pt, over 20CSO2Co electrolyte. Several aspects should be remarked. Though some differences were obtained for different cathode materials, in all the samples were observed important variations of interface polarization with current density. However the electrode resistance does not decrease with the supply of DC current in all the range of current and temperature. In most of results the electrode polarization increases for low values of current densities, achieving a maximum and then decreasing for higher values of current fluxes. Nevertheless the maximum of resistance is displaced towards higher values of current when the temperature increases. This makes that at high temperatures (900 and 850 °C) the best electrode performances are obtained for low values of current flux (or even for OCV conditions). On the other hand, important improvements of electrode performance were obtained for high current fluxes at low temperatures (700 and 750 °C). Also one should remark that the clear increase in performance with temperature obtained in OCV conditions and for low values of current density is less important at high density fluxes. Similar behaviour and performance were obtained for cathodes of La_2NiO_4 and $La_3Ni_2O_7$, whereas Pt electrode clearly possesses the worst performance. Some differences were obtained when using La_2NiO_4–20CSO com-

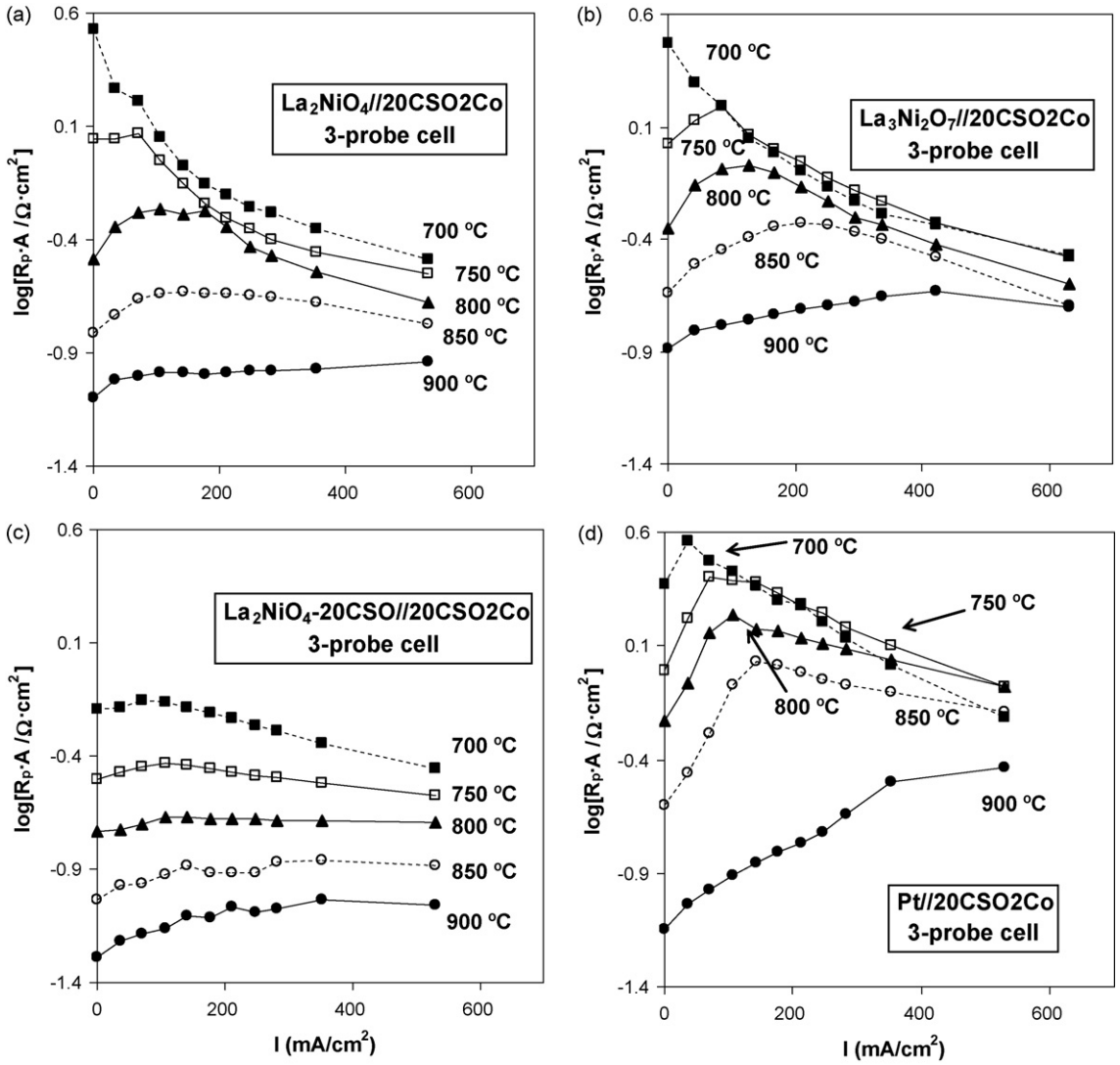

Fig. 9. Interface polarization as a function of cathodic DC current in the range of 700–900 °C for (a) La_2NiO_4, (b) $La_3Ni_2O_7$, (c) La_2NiO_4–20CSO and (d) Pt as cathode materials over 20CSO2Co electrolytes.

posite as cathode. Though the OCV polarization resistance is clearly lower than that of pure cathodes, it is remarkable that the current density does not produce high changes in the values of electrode resistance of composite material. This makes that the performances obtained at high values of current fluxes are very similar for both pure La_2NiO_4 and La_2NiO_4–20CSO composite (Fig. 9(a) and (c)). Some studies previously reported for LSM-based cathodes on YSZ or ceria-based electrolytes revealed that the electrode performance was enhanced after cathodic polarization. Several authors suggested that the improvement of the performance was associated to the partial reduction of Mn^{3+} to Mn^{2+} at the bulk or on the surface of LSM [14,31,32] with concomitant generation of oxygen vacancies. This increase in the surface oxygen vacancies would promote the oxygen dissociation and adsorption thus decreasing the interfacial resistance [6,14]. The obtained reduction of the low-frequency arc in the polarization process under cathodic current [14,31,33], could indicate that the O^{2-} surface diffusion close to the "triple phase boundary" is enhanced.

Our results indicate that the increase in the current flux does not systematically increase the electrode performance of the studied cathodes (Fig. 9), suggesting a minimum value of current density to obtain improvements of the performance. This kind of behaviour was also obtained for LSM/YSZ cathode on YSZ electrolyte [10]. The ionic conduction of O^{2-} in La_2NiO_4 and $La_3Ni_2O_7$-based materials takes place by a combined mechanism of oxygen vacancy diffusion in the perovskite planes and interstitial anion migration in the rock-salt layers [34]. This seems to eliminate the possibility to relate the improvement of electrode performance for high current fluxes, with any partial reduction of Ni^{3+} to Ni^{2+}. Another important feature is the fact that the interface resistance is diminished by both cathodic and anodic high current polarization. Also it is important to clarify that the electrode performance is changed when applying cathodic polarization during the measurement, but the starting behaviour is practically recovered when coming back to OCV conditions. It is of standing out that the electrode polarization for Pt-electrode also reveals clear variations with current fluxes (Fig. 9). These results suggest that the generation of vacancies at the cathode, coming from possible partial reduction of cations, is not the only factor to affect the changes in interface polarization with cathodic DC current fluxes.

At high temperature (900 °C), Fig. 9 shows that the polarization resistance increases with the current flux, for all the studied samples. When DC current is applied, the oxygen vacancies at the surface cathode/electrolyte could be easily removed given that the

oxygen reduction is favoured at high temperature. As consequence the electrode polarization resistance should be harmed. At 850 °C the situation is similar for low current fluxes, however the oxygen reduction at the interface surface begins to be less favoured. As consequence, the vacancies removed from the interface are replaced by new vacancies, coming from the electrolyte, for a given value of current flux. For higher values of DC current, the vacancies at the interface begin to increase with the current flux, which produces the decrease in the electrode polarization. For very high current fluxes, the problems coming from the oxygen gas diffusion smooth the decrease in the electrode resistance. If temperature decreases the electrode polarization behaviour reaches the maximum at lower values of current density. Even, for sufficiently low temperature the supply of DC current could systematically increase the oxygen vacancies at the interface because of the greater difficulty in the remove of oxygen vacancies by the oxygen reduction reaction. These kinds of behaviour were obtained for all the studied samples, even for Pt-electrode (Fig. 9). However appreciable differences were obtained coming from different interface nature. Composite based on La_2NiO_4–20CSO clearly possesses the best electrode performance in OCV conditions of all the studied materials, given that the introduction of the 20CSO ionic-conduction-phase increases the active sites of reaction. However the effect of DC current is less important compared with the other samples. The main reason could be due to the fact that interface oxygen vacancies, coming from the DC current through the electrolyte, are easily removed by the ionic conduction in the cathode. This makes that the increase in the DC current produces only small changes in the oxygen vacancies concentration at the interface, and as consequence the electrode polarization is less affected. For La_2NiO_4 and $La_3Ni_2O_7$ the surface oxygen vacancies concentration could more easily be changed with DC current, given that they possess small ionic conductivity, whereas for Pt-electrode the total absence of ionic conduction reinforces this behaviour (Fig. 9) and the current flux highly affects the interface properties.

To analyze the effect of the history on the interface polarization of different cathode materials, we proceeded as follows: firstly impedance spectroscopy at 800 °C was performed in OCV conditions; then a DC cathodic current flux of 354 mA cm^{-2} was applied between the working and counter electrodes for 10, 20 and 40 min and impedance spectroscopy in OCV conditions was performed again after interrupting each DC current flux. Fig. 10 shows the impedance spectra obtained for cathodes of $La_3Ni_2O_7$, La_2NiO_4, La_2NiO_4–20CSO and Pt, deposited onto the 20CSO2Co electrolyte. Firstly it is observed that after applying 354 mA cm^{-2} for 10 min, OCV impedance measurements reveal that the electrode polarization recovers the original nonpolarized state for ceramic cathodes, but it is enhanced for Pt electrodes. Then, the Pt-sample was retained in air and OCV conditions and impedance measurements indicated that the electrode polarization was increasing with time to finally obtain the starting value (previous to the current supply). After 20 min of DC cathodic polarization in the working electrode, not only Pt-electrode sample is now enhanced in OCV conditions, but also La_2NiO_4 and $La_3Ni_2O_7$ samples. However, whereas the decrease in the electrode polarization of ceramic cathodes is similar, it is clearly more important in Pt electrodes. In addition the composite electrode is not affected by the previous current flux. After 40 min of DC cathodic current the decrease in the interface resistance is also more important in Pt electrodes than in La_2NiO_4 and $La_3Ni_2O_7$, and the composite is again practically not affected by the previous history. These results indicate that the effect of the history on the electrode polarization is clearly dependent on the nature of the cathode material, in a similar way as it was commented before. For pure electronic cathode, as Pt electrode, the

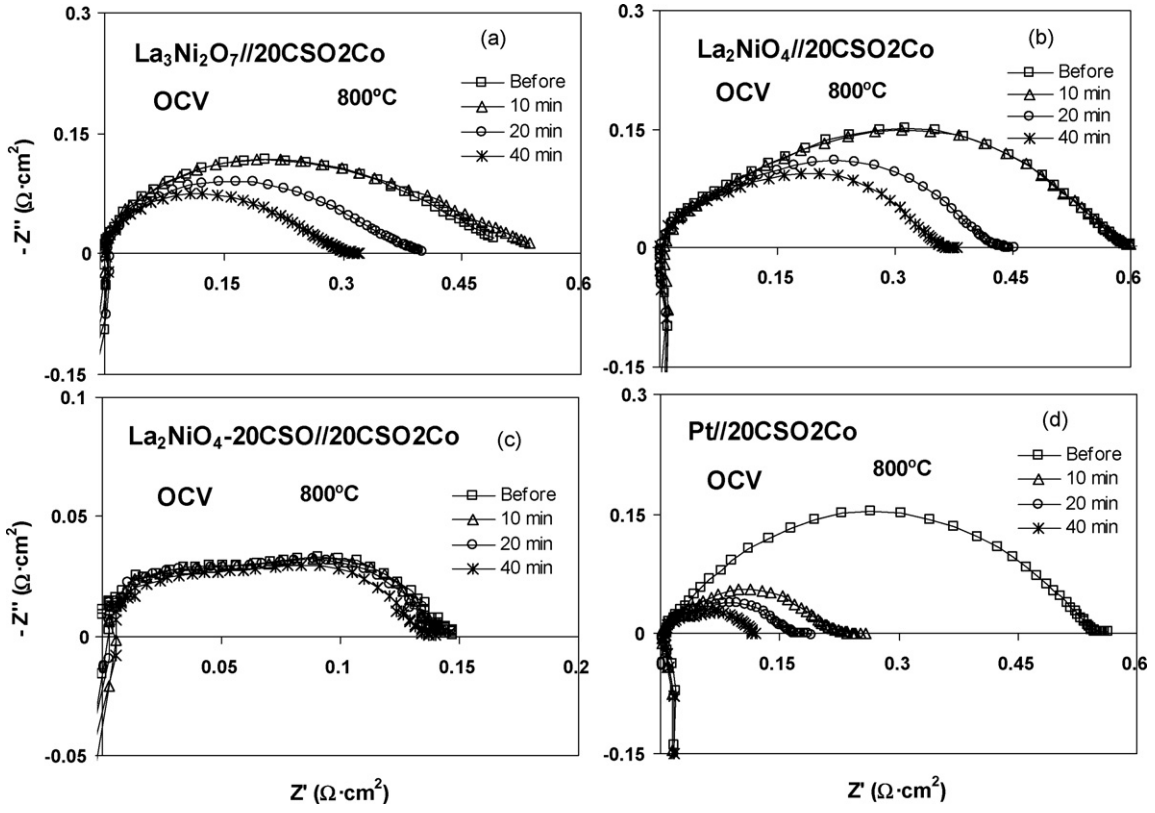

Fig. 10. Electrode polarization at 800 °C in OCV conditions before and after a cathodic DC current flux of 354 mA cm^{-2} during 10, 20 and 40 min, for La_2NiO_4 (a), $La_3Ni_2O_7$ (b), La_2NiO_4–20CSO (c) and Pt (d).

application of DC current flux strongly affects the later OCV interface resistance, even for short periods of application. For samples with some ionic conductivity as La_2NiO_4 and $La_3Ni_2O_7$ cathodes, the OCV interface resistance is less decreased after the same periods of DC current fluxes. Finally for composite with high ionic conductivity, the previous DC current flux on the sample has no important effect on the OCV interface resistance. When the working electrode is DC-cathodically polarized for a time, the oxygen vacancies coming from the electrolyte go towards the interface of the electrolyte with the working electrode. If the cathode material is pure electronic conductor, as occurs with Pt electrode, the vacancies are only removed by the oxygen electrochemical reaction at the interface. This makes that after long periods of relatively high DC current flux ($354\,mA\,cm^{-2}$) there is an important accumulation of vacancies at the interface. As consequence, in OCV conditions, after this current fluxing, there are more places of reaction which decrease the interface resistance. On the other hand, if the cathode material possesses a high ionic conductivity, as it is the case of the composite La_2NiO_4–20CSO, when the DC current is fluxing the oxygen vacancies at the interface are easily removed by the ionic conduction of the cathode. This makes that there are practically no accumulation of vacancies at the interface, and as consequence when the current is interrupted the OCV interface resistance is practically similar to the previous one obtained before the current flux. For La_2NiO_4 and $La_3Ni_2O_7$, the obtained behaviour is consequent with their low ionic conductivity, and the applied DC current for a time affects the later OCV measurements in a minor way than in the Pt electrode.

In order to analyze the evolution of the interfacial resistance we also studied the effect of anodic DC current polarization after being cathodically polarized. Firstly, impedance spectroscopy was performed in OCV conditions, without any current passing through the samples. Fig. 11 shows that the interface resistance of the cathode $La_3Ni_2O_7$ onto 20CSO2Co electrolyte before passing any DC current possesses a value of $0.86\,\Omega\,cm^2$. Note that this value is sensibly higher than that obtained in Fig. 5 for the same system ($0.46\,\Omega\,cm^2$), because the current experiment was performed after the sample was submitted at 800 °C for 1 day. This produced an important decrease in the OCV electrode performance, mainly due to the coarsening of Pt current collectors. After supplying a cathodic DC current flux of $420\,mA\,cm^{-2}$ during 120 min, the interface polarization of $La_3Ni_2O_7$ in OCV conditions was enhanced to $0.25\,\Omega\,cm^2$ (Fig. 11). This value of interface resistance in OCV conditions was quite similar to that previously obtained by impedance spectroscopy with a simultaneously DC cathodic current flux of $420\,mA\,cm^{-2}$ ($0.28\,\Omega\,cm^2$, Fig. 6, open squares). This indicates that

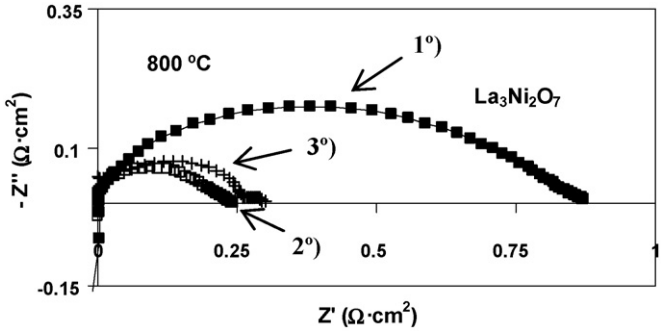

Fig. 11. Impedance spectra obtained at 800 °C for $La_3Ni_2O_7$ cathode with 20CSO2Co electrolyte. Spectra were obtained: (1°) in OCV conditions, before DC current aging (closed squares); (2°) in OCV conditions after a cathodic current flux of $420\,mA\,cm^{-2}$ during 120 min (open squares); and (3°) with simultaneous DC cathodic current of $420\,mA\,cm^{-2}$, after DC current aging (crosses).

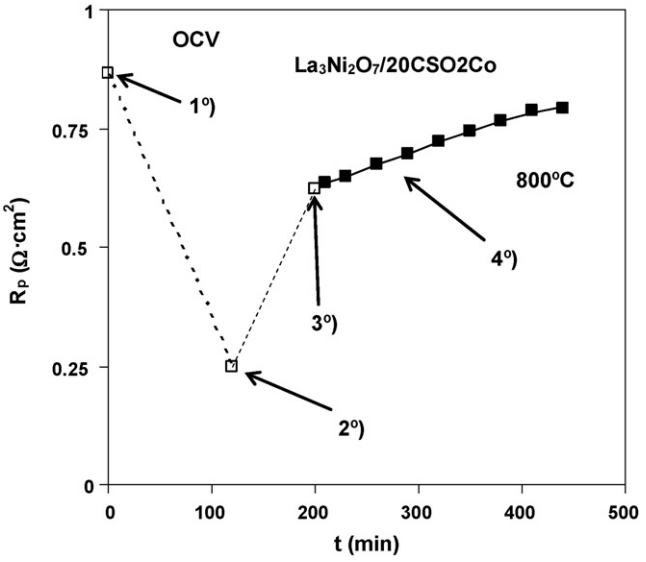

Fig. 12. Electrode polarization for $La_3Ni_2O_7$/20CSO2Co 3-probe semi-cell at 800 °C in OCV conditions. Measurements were obtained in the following conditions: (1°) before any DC current flux; (2°) after 120 min of $420\,mA\,cm^{-2}$ DC cathodic polarization on the working electrode; (3°) after 80 min of $420\,mA\,cm^{-2}$ of DC anodic polarization on the working electrode; and (4°) after steps 2° and 3° without any DC current flux as a function of time.

the electrode polarization obtained when DC current is fluxing is now retained in OCV conditions after the current is applied for a long time (120 min). Moreover, impedance spectroscopy performed with simultaneous flux of $420\,mA\,cm^{-2}$ (after DC current aging) showed that the electrode polarization with current flux is practically non affected by the history of the sample, given that it is very similar to that obtained before the aging process (Fig. 11). After that, an anodic polarization current of $420\,mA\,cm^{-2}$ was applied for 80 min and the performance in OCV was spoiled to $0.62\,\Omega\,cm^2$ (Fig. 12). These results indicate that the previous cathodically polarized electrode seems to be reversible with the anodic polarization and the interface resistance goes towards the original value. Then, the sample was retained in OCV conditions and the performance was analyzed as a function of time. Fig. 12 reveals that the interface resistance in OCV conditions systematically increased with an estimated rate of $0.04–0.05\,\Omega\,cm^2\,h^{-1}$. This made that the electrode resistance in OCV conditions was progressively increased from 0.62 to $0.79\,\Omega\,cm^2$ in 4 h.

In order to obtain reliable values of electrode overpotential, we analyzed the electrode polarization resistance as a function of DC current flux, both before and after DC current polarization for a relatively long time. For this purpose, we performed impedance spectroscopy with simultaneous cathodic DC current fluxes between 0 and $530\,mA\,cm^{-2}$; then the samples were submitted to a cathodic DC current flux of $354\,mA\,cm^{-2}$ for 80 min, and after that impedance spectroscopy with simultaneous DC current fluxes were performed again. Fig. 13(a) shows the results of interface resistance obtained at 700 and 800 °C for cathode La_2NiO_4 with 20CSO2Co electrolyte. It is observed that the DC polarization does not produce important changes in the electrode performance behaviour at intermediate and high current fluxes. For low values of DC current flux the electrode performance is retained higher after being cathodically polarized at $354\,mA\,cm^{-2}$ for 80 min. However when current flux is increasing differences vanish and the electrode performance is practically non-affected by the history. As consequence the non-linear behaviour of the electrode overpotential (Fig. 13(b)) obtained before DC polarization is also reproduced after the current flux aging. This has important advantages to use

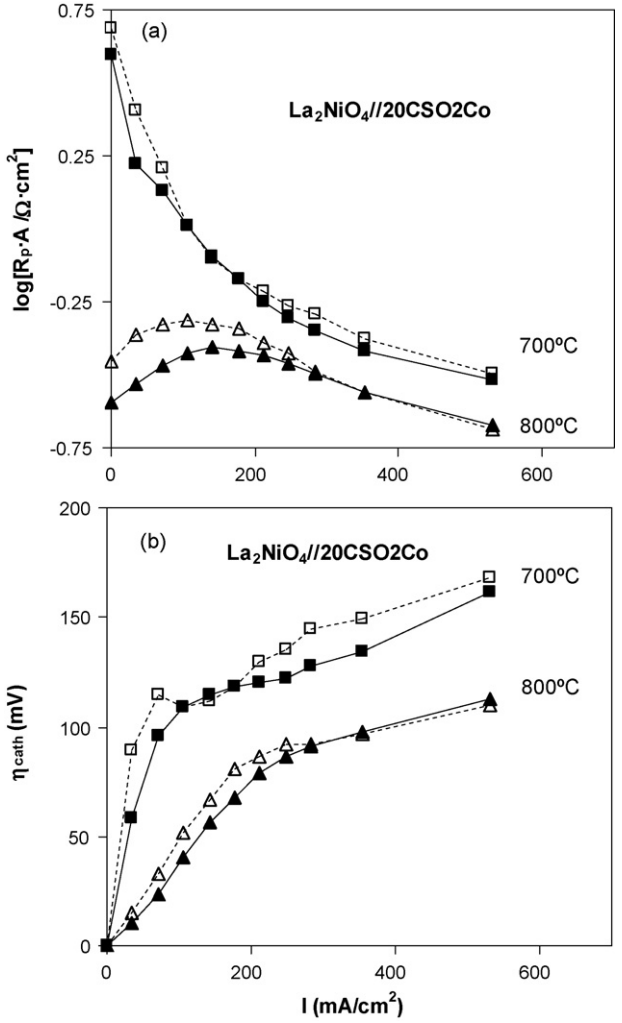

Fig. 13. Interface resistance (a) and cathode overpotential (b) as a function of cathodic DC current density for La_2NiO_4/20CSO2Co system extracted from results of impedance spectroscopy. Closed symbols correspond to results obtained after applying $-354\,mA\,cm^{-2}$ for 80 min, whereas open symbols correspond to results obtained before polarization.

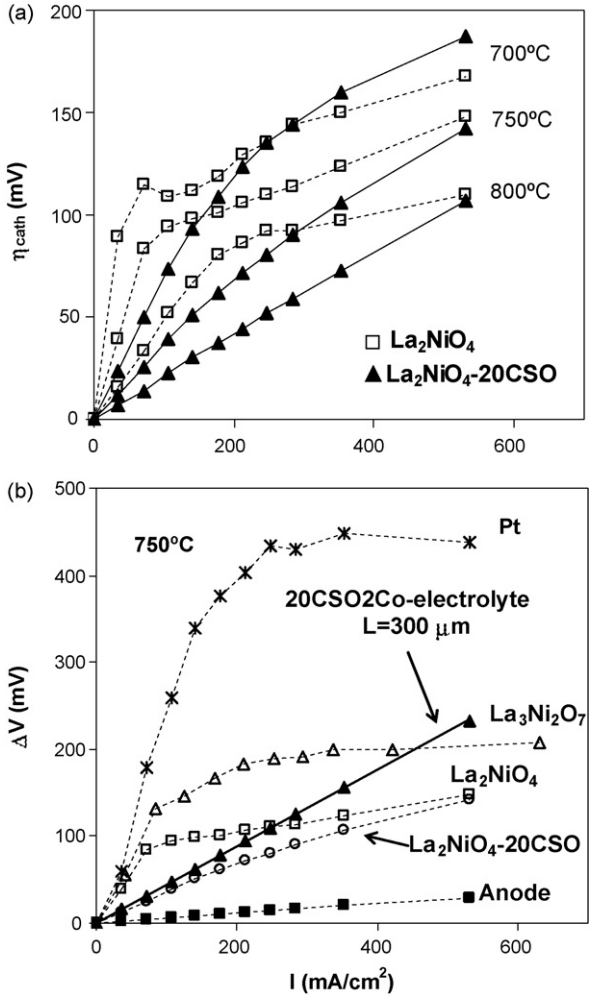

Fig. 14. (a) Cathode overpotential as a function of current flux and temperature for La_2NiO_4 and La_2NiO_4–20CSO. (b) Voltage losses in cathode, anode and electrolyte at 750 °C for La_2NiO_4, $La_3Ni_2O_7$, La_2NiO_4–20CSO and Pt as cathodes over 20CSO2Co electrolyte (300 μm in thickness), and Ni–20CSO as anode [35].

the materials in SOFC systems at intermediate or relatively high current fluxes, given that the electrode overpotential is retained around 110 and 160 mV for 800 and 700 °C, respectively, for current fluxes as high as $530\,mA\,cm^{-2}$.

On the other hand, the use of composite produces a clear decrease in the cathode overpotential due to the decrease in the interface resistance (Fig. 9), only for low and intermediate values of current fluxes (Fig. 14(a)). However the electrode overpotential is practically similar for both La_2NiO_4-pure and La_2NiO_4–20CSO-composite at high values of current fluxes. This surprising behaviour comes from the fact that the composite electrode performance is practically not influenced by the DC current flux (Fig. 9) whereas the electrode performance of La_2NiO_4-pure cathode is enormously improved for high values of current flux at intermediate temperature. Fig. 14(b) reveals that the cathode overpotential is retained below the electrolyte ohmic loss (with an electrolyte thickness of 300 μm) in the entire range of current fluxes for La_2NiO_4–20CSO composite, and also for La_2NiO_4 pure cathode at intermediate and high current fluxes. It is to note that La_2NiO_4 and $La_3Ni_2O_7$ materials present similar overpotential behaviour, but the slightly better performance obtained by the first one at 750 °C produced lower cathode overpotential. Moreover, the cathode overpotential of Pt electrodes is 2–4 times higher than that obtained for the studied ceramic cathode materials.

The knowledge of the cathode overpotential behaviour as function of current load (I) allows to obtain estimations of the cell voltage (E) and power (P), according to Eqs. (1) and (2):

$$E = \mathrm{OCV} - I \cdot (R_s + R_{p,cath} + R_{p,anod}) \quad (1)$$

$$P = I \cdot \mathrm{OCV} - I^2 \cdot (R_s + R_{p,cath} + R_{p,anod}) \quad (2)$$

where R_s, $R_{p,cath}$ and $R_{p,anod}$ are the values of resistance of electrolyte, cathode and anode respectively, for the corresponding value of current flux (I).

For this purpose we estimated values of anode overpotential from data of Ref. [35] for a Ni–20CSO anode operating with 20CGO ($Ce_{0.8}Gd_{0.2}O_{2-\delta}$) electrolyte using H_2 fuel with 10% H_2O. The losses of the 20CSO2Co electrolyte with 300 μm in thickness were extracted from data of electrolyte conductivity (Fig. 7), and the open circuit voltage of the cell was calculated from data of electronic transport number of the electrolyte averaged to the fuel and air sides of the cell ($t_{e,av}$), as we previously reported [19], according to Eq. 3:

$$\mathrm{OCV}_{mix} = \mathrm{OCV}(1 - t_{e,av}) \quad (3)$$

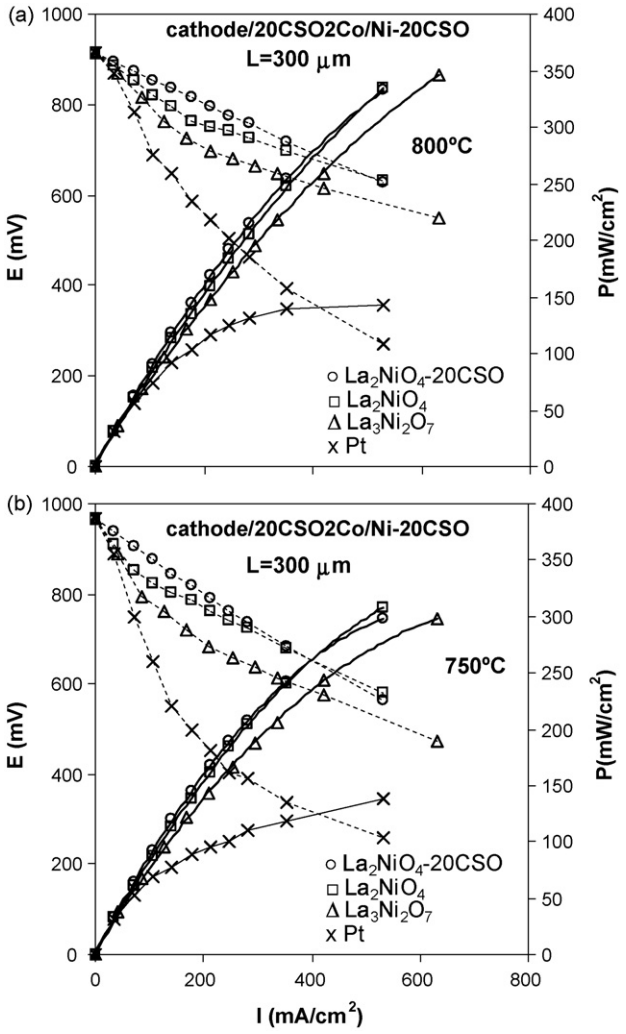

Fig. 15. Estimated cell voltage (dashed lines) and power density (straight lines) as function of current flux at 800 °C (a) and 750 °C (b). Data were obtained from values of cathode overpotential and electrolyte loss for a 300 μm electrolyte thickness, for La_2NiO_4, $La_3Ni_2O_7$, La_2NiO_4–20CSO and Pt as cathodes over 20CSO2Co electrolyte, and using the anode overpotential (Ni–20CSO anode) extracted from data of Ref [35].

Note that Eq. (3) relates the open circuit voltage of a mixed conducting electrolyte (OCV_{mix}) (as ceria-based material) with the open circuit voltage of an ideal ionic conductor (OCV) (extracted from Nernst equation).

The good performance of the cathodes makes possible to estimate values of maximum power density around 400 mW cm^{-2} at 800 °C, and around 300–350 mW cm^{-2} at 750 °C, for current load of 800 mA cm^{-2} for composite and pure ceramic cathodes (Fig. 15). These results suggest the possibility of use La_2NiO_4 and $La_3Ni_2O_7$-based materials as cathodes in Intermediate Solid Oxide Fuel Cells.

4. Conclusions

Impedance spectroscopy was employed to analyze the electrode performance of La_2NiO_4 and $La_3Ni_2O_7$ systems in OCV conditions and with simultaneous DC current polarization. Results obtained in symmetrical configuration agree well with those obtained in 3-probe set-up in OCV conditions, but not under DC current fluxes. The electrode performance of the studied materials over $Ce_{0.8}Sm_{0.2}O_{2-\delta}$ + 2%Co electrolyte is dependent on the current flux and direction. Different performances were obtained under cathodic and anodic DC polarization. For high temperatures, the interfacial resistance increases with DC current for low fluxes and then decreases for high fluxes. When temperature decreases the maximum of resistance is reached for lower current fluxes and the effect of the performance improvement at high currents is clearly more appreciated. The study was extended to La_2NiO_4–$Ce_{0.8}Sm_{0.2}O_{2-\delta}$ composite and Pt as cathode materials. The introduction of the ionically conducting phase increases the electrode performance in OCV conditions and it is only slightly affected by current flux. However, the use of pure electronic cathode (Pt) harms the electrode performance in OCV conditions and it is highly affected by the current flux. For Pt, La_2NiO_4 and $La_3Ni_2O_7$ materials the electrode performance under current flux is affected by the history for low values of current flux but not for high fluxes. Nevertheless, La_2NiO_4–$Ce_{0.8}Sm_{0.2}O_{2-\delta}$ composite is practically not affected by the history in the whole range of current fluxes studied in this work. The dependence of electrode overpotential on current flux is practically lineal for composite material whereas in pure materials are observed important deviations from linearity at high current fluxes. Performances of 300–50 mW cm^{-2} for 800 mA cm^{-2} are estimated for pure and composite ceramic electrodes at 750 °C operating with $Ce_{0.8}Sm_{0.2}O_{2-\delta}$ + 2Co electrolyte with 300 μm in thickness and Ni–$Ce_{0.8}Sm_{0.2}O_{2-\delta}$ composite as anode and H_2 as fuel. These results place La_2NiO_4 and $La_3Ni_2O_7$-based materials as candidates to be used as cathodes in Intermediate Solid Oxide Fuel Cells.

Acknowledgements

The work was sponsored by the Community of Madrid (ENERCAM-CM; S-0505/ENE/0304) and the Spanish Innovation and Science Ministry (MATSOFC; MAT2005-02933). One of the authors (D.P.-C.) is also grateful to the Spanish Innovation and Science Ministry for financial support by means of the "Juan de la Cierva" program.

References

[1] B.C.H. Steele, Solid State Ionics 134 (1–2) (2000) 3.
[2] J.W. Fergus, J. Power Sources 162 (2006) 30.
[3] M. Shiono, Kenichi Kobayashi, T.L. Nguyen, K. Hosoda, T. Kato, K. Ota, M. Dokiya, Solid State Ionics 170 (2004) 1.
[4] B.C.H. Steele, K.M. Hori, S. Uchino, Solid State Ionics 135 (2000) 445.
[5] C.R. Xia, M.L. Liu, Adv. Mater. 14 (2002) 521.
[6] X. Xu, C. Xia, G. Xiao, D. Peng, Solid State Ionics 176 (2005) 1513.
[7] T. Kenjo, S. Osawa, K. Fujikawa, J. Electrochem. Soc. 138 (1991) 349.
[8] F.S. Baumann, J. Fleig, H.-U. Habermeier, J. Maier, Solid State Ionics 177 (2006) 1071.
[9] M.J. Jørgensen, M. Mogensen, J. Electrochem. Soc. 148 (5) (2001) A433.
[10] S. McIntosh, S.B. Adler, J.M. Vohs, R.J. Gorte, Electrochem. Solid State Lett. 7 (2004) A111.
[11] J.M. Ralph, A.C. Schoeler, M. Krumpelt, J. Mater. Sci. 36 (2001) 1161.
[12] J.-W. Kim, A.V. Virkar, K.-Z. Fung, K. Mehta, S.C. Singhal, J. Electrochem. Soc. 146 (1999) 69.
[13] S.P. Jiang, J.G. Love, J.P. Zhang, M. Hoang, Y. Ramprakash, A.E. Hughes, S.P.S. Badwal, Solid State Ionics 121 (1999) 1.
[14] X.J. Chen, K.A. Khor, S.H. Chan, Solid State Ionics 167 (2004) 379.
[15] V.V. Kharton, A.P. Viskup, E.N. Naumovich, F.M.B. Marques, J. Mater. Chem. 9 (1999) 2623.
[16] J.A. Kilner, C.K.M. Shaw, Solid State Ionics 154–155 (2002) 523.
[17] F. Mauvy, J.M. Bassat, E. Bohem, J.P. Manuad, P. Dordor, J.C. Grenier, Solid State Ionics 158 (2003) 17.
[18] A. Aguadero, J.A. Alonso, M.J. Martínez-Lope, M.T. Fernández-Díaz, M.J. Escudero, L. Daza, J. Mater. Chem. 16 (2006) 3402.
[19] D. Pérez-Coll, A. Aguadero, M.J. Escudero, P. Núñez, L. Daza, J. Power Sources 178 (2008) 151.
[20] G. Amow, I.J. Davidson, S.J. Skinner, Solid State Ionics 177 (2006) 1205.
[21] G. Amow, P.S. Whitfield, I.J. Davidson, R.P. Hammond, C.N. Munnings, S.J. Skinner, Ceram. Int. 30 (2004) 1635.
[22] M.D. Carvalho, F.M.A. Costa, I.D. Pereira, A. Wattiaux, J.M. Bassat, J.C. Grenier, M. Pouchard, J. Mater. Chem. 7 (1997) 2107.
[23] T. Roisnel, J. Rodríguez-Carvajal, WinPLOTR: a Windows tool for powder diffraction patterns analysis, in: R. Delhez, E.J. Mittenmeijer (Eds.), Proceedings of the

Seventh European Powder Diffraction Conference (EPDIC 7), Materials Science Forum, 2000, p. 118.
[24] J. Rodríguez-Carvajal, Phys. B 192 (1993) 55.
[25] C. Kleinlogel, L.J. Gauckler, Solid State Ionics 135 (2000) 567.
[26] D.P. Fagg, J.C.C. Abrantes, D. Pérez-Coll, P. Núñez, V.V. Kharton, J.R. Frade, Electrochim. Acta 48 (2003 1023).
[27] S.B. Adler, B.T. Henderson, M.A. Wilson, D.M. Taylor, R.E. Richards, Solid State Ionics 134 (2000) 35.
[28] M. Zinkevich, F. Aldinger, J. Alloys Compd. 375 (2004) 147.
[29] F. Mauvy, C. Lalanne, J.-M. Bassat, J.-C. Grenier, H. Zhao, L. Huo, P. Stevens, J. Electrochem. Soc. 153 (8) (2006) A1547.
[30] G. Fafilek, Solid State Ionics 176 (2005 2023).
[31] E. Siebert, A. Hammouche, M. Kleitz, Electrochim. Acta 40 (1995) 1741.
[32] H.Y. Lee, W.S. Cho, S.M. Oh, H.-D. Wiemhöfer, W. Göpel, J. Electrochem. Soc. 142 (1995) 2659.
[33] B. Gharbage, T. Pagnier, A. Hammou, J. Electrochem. Soc 141 (1994) 2118.
[34] V.V. Kharton, A.A. Yaremchenko, A.L. Shaula, M.V. Patrakeev, E.N. Naumovich, D.I. Logvinovich, J.R. Frade, F.M.B. Marques, J. Solid State Chem. 177 (2004) 26.
[35] S. Wang, T. Kato, S. Nagata, T. Kaneko, N. Iwashita, T. Honda, M. Dokiya, Solid State Ionics 152–153 (2002) 477.